Evidence of a common mechanism of disassembly of adherens junctions through Gα13 targeting of VE-cadherin

Haixia Gong, Xiaopei Gao, Shaoting Feng, M. Rizwan Siddiqui, Alexander Garcia, Marcelo G. Bonini, Yulia Komarova, Stephen M. Vogel, Dolly Mehta, and Asrar B. Malik

Department of Pharmacology and the Center for Lung and Vascular Biology, University of Illinois, Chicago, Il 60612

The heterotrimeric G protein Gα13 transduces signals from G protein–coupled receptors (GPCRs) to induce cell spreading, differentiation, migration, and cell polarity. Here, we describe a novel GPCR–independent function of Gα13 in regulating the stability of endo-thelial cell adherens junctions (AJs). We observed that the oxidant H_2O_2, which is released in response to multiple proinflammatory mediators, induced the interaction of Gα13 with VE-cadherin. Gα13 binding to VE-cadherin in turn induced Src activation and VE-cadherin phosphorylation at Tyr 658, the p120-catenin binding site thought to be responsible for VE-cadherin internalization. Inhibition of Gα13–VE-cadherin interaction using an interfer-ing peptide derived from the Gα13 binding motif on VE-cadherin abrogated the disruption of AJs in response to inflammatory mediators. These studies identify a unique role of Gα13 binding to VE-cadherin in mediating VE-cadherin internalization and endothelial barrier disruption and inflammation.

CORRESPONDENCE
Asrar B. Malik:
abmalik@uic.edu

Abbreviation used: AJ, adherens junction; CD, cytoplasmic do-main; CKO, conditional KO; CLP, cecal ligation and punc-ture; DPI, diphenyleneiodo-nium; HMVEC-L, human lung microvascular endothelial cell; NAC, *N*-acetyl-L-cysteine; TER, transendothelial electrical resistance; WB, Western blot.

The assembly of adherens junctions (AJs) is re-quired for maintenance of normal endothelial barrier function, whereas disassembly in response to a variety of inflammatory mediators induces vascular barrier leakiness and transendothelial migration of inflammatory cells, leading to in-flammation (Dejana et al., 2008; Komarova and Malik, 2010). Endothelial permeability is essen-tial for the pathogenesis of acute and chronic in-flammation underlying many diseases (Komarova et al., 2007), including atherosclerosis (Correale and Villa, 2007), cancer (Kim et al., 2009), and acute lung injury (Komarova et al., 2007). The understanding of signaling pathways that orches-trate the assembly and disassembly of AJs is re-quired to provide insights into the molecular regulation of endothelial permeability and the potential ability to control excessive vascular leakiness. Catenins are the primary VE-cadherin binding partners, and they determine the stabil-ity of AJs (Komarova and Malik, 2010). c-Src–dependent phosphorylation of VE-cadherin at Tyr 658 induced uncoupling of p120-catenin from VE-cadherin, resulting in internalization of VE-cadherin from AJs and subsequent loss of en-dothelial barrier function (Xiao et al., 2003; Potter et al., 2005; Hatanaka et al., 2011). Expression of

constitutively active Src, but not the dominant negative c-Src tyrosine kinase (CSK), a negative regulator of c-Src (Okada et al., 1991; Cole et al., 2003; Huang et al., 2009), also increased endo-thelial permeability (Adam et al., 2010). Gα13, the Gα12 subfamily member of heterotrimeric G proteins, like other G proteins, responds to GPCR activation by interacting with down-stream effectors (Kozasa et al., 1998; Brown et al., 2006). Gα13 has been shown to regulate the processes of cell differentiation, retraction, mi-gration, and platelet shape change, as well as endothelial permeability, through RhoA activa-tion (Offermanns et al., 1997; Klages et al., 1999; Holinstat et al., 2003). In addition, Gα13 appears to be exceptional, as it was shown to have other key functions independent of GPCR coupling (Shan et al., 2006; Kelly et al., 2007). Gα13 was shown to mediate β3 integrin outside–in sig-naling that induced cell spreading through inhi-bition of RhoA (Gong et al., 2010). Gα13 also mediated receptor tyrosine kinase signaling to

The Rockefeller University Press $30.00
J. Exp. Med. 2014 Vol. 211 No. 3   579–591
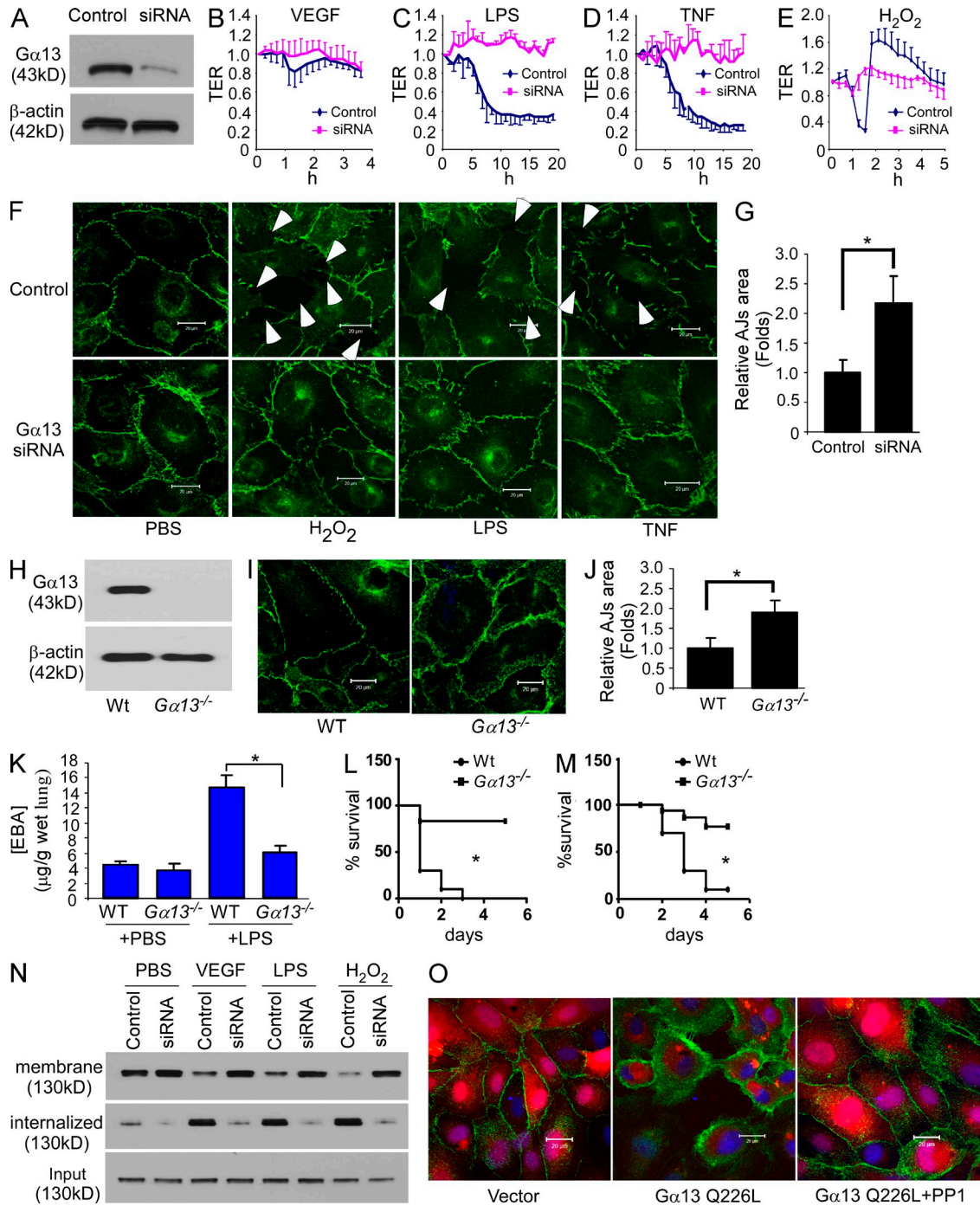www.jem.org/cgi/doi/10.1084/jem.20131190

579

Figure 1. **Gα13 binding to VE–cadherin induces endothelial barrier disruption at the level of AJ.** (A) HMVEC-L cells were infected with control siRNA and Gα13 siRNA lentivirus, and Gα13 expression was assessed by Western blotting (WB). Figures are representative of four experiments. (B–E) Confluent HMVEC-L cells infected with control siRNA or Gα13 siRNA lentivirus were stimulated with 20 ng/ml VEGF (B), 2 µg/ml LPS (C), 20 ng/ml TNF (D), and 300 µM H_2O_2 (E), and transendothelial electrical resistance (TER) was measured. TER values of each monolayer were normalized to their basal level values. Data are expressed as mean ± SD (n = 3–4 in each group). Data are representative of 2–3 experiments. (F) Gα13 siRNA lentivirus-infected confluent HMVEC-L cells were stimulated with 300 µM H_2O_2, 2 µg/ml LPS, or 20 ng/ml TNF, and then analyzed by confocal microscopy. Green indicates labeling of VE-cadherin. Bars, 20 µM. Figures are representative of three experiments. (G) Quantification of AJ area from three randomly chosen areas from the images in F (mean ± SD). *, P < 0.01. Figures are representative of two experiments. (H) PMECs isolated from WT (129/B6) and *Gna13flox/flox* mice were infected with Cre recombinase adenovirus to induce Gα13 deletion. VE-cadherin expression was analyzed by WB; the experiment was done twice. (I) PMECs isolated from WT (129/B6) and *Gna13flox/flox* mice were infected with Cre recombinase adenovirus, and VE-cadherin expression was analyzed by confocal microscopy. Green indicates VE-cadherin. Bar, 20 µM. Figures are representative of two experiments. (J) Quantification of AJ area in (I) from

promote cell migration (Shan et al., 2006). Gα13 additionally regulated angiogenesis through induction of VEGFR2 expression (Sivaraj et al., 2013). Gα13 through binding to E-cadherin in epithelial cells mediated translocation of β-catenin from junctions to the nucleus resulting in β-catenin-mediated transcription activation (Kaplan et al., 2001; Turm et al., 2010).

In this study, we identified a previously unrecognized role of Gα13 in mediating the disassembly of VE-cadherin junctions and increasing endothelial permeability. We demonstrated that interaction of Gα13 and VE-cadherin activated in response to several proinflammatory ligands induced Src-dependent VE-cadherin phosphorylation at Tyr 658, the p120-catenin binding site responsible for VE-cadherin internalization, resulting in VE-cadherin junction disassembly.

RESULTS

Gα13 regulates VE–cadherin–dependent endothelial barrier function

To address the role of Gα13 in regulating endothelial barrier function, we first studied the effects of depletion of Gα13 by siRNA in human lung microvascular endothelial cells (HMVEC-L; Fig. 1 A). Gα13 depletion, but not Gα12 depletion, prevented endothelial barrier disruption induced by several diverse non–GPCR agonists, VEGF, the bacterial lipid LPS, TNF, and oxidative stress H_2O_2 (Fig. 1, B–F; and not depicted). Gα13 depletion also increased VE-cadherin localization at AJs (Fig. 1, F and G). The same phenotype was evident in Gα13 knockout mouse pulmonary microvascular endothelial cells (PMEC; Fig. 1, H–J). Deletion of Gα13 also made the endothelial junctional barrier more resistant to the disruptive effects of mediators like LPS, such that deletion of Gα13 in endothelial cells was shown to prevent LPS–induced increase in transvascular permeability of albumin in lung microvessels in vivo (Fig. 1 K). The more resistant vascular endothelial barrier of these mice also contributed to reduced mortality in response to LPS and the cecal ligation and puncture (CLP) model of sepsis (Fig. 1, L and M).

Gα13 depletion strengthens AJs by inhibiting VE-cadherin internalization

As VE-cadherin stabilization at AJs is required for the integrity of endothelial AJs (Chiasson et al., 2009), we next addressed the possibility that Gα13 regulated integrity of AJs by controlling the process of VE-cadherin internalization, which is believed to be important in mediating AJ disassembly (Gavard and Gutkind, 2006; Gavard et al., 2008). To address this concept, we determined whether Gα13 was required for internalization of VE-cadherin from AJs. By separating cell surface and internalized biotinylated proteins using streptavidin-conjugated agarose beads (Wu et al., 2005), Gα13 depletion was shown to increase cell surface VE-cadherin localization and to decrease the amount of internalized VE-cadherin (Fig. 1 N).

Because these findings suggest a key role of Gα13 in mediating disruption of AJs, we next queried whether expressing constitutively active GTPase-deficient Gα13 (Gα13 Q226L) mutant would itself dissemble AJs. We observed here that expression of Gα13 Q226L in endothelial cells induced VE-cadherin internalization and disrupted AJs (Fig. 1 O and not depicted), responses that were rescued by the Src kinase inhibitor PP1 (Fig. 1 O and not depicted). Significant VE-cadherin internalization was also evident in HMVEC-L expressing Gα13 C-terminal 5-aa truncation mutant (Gα13-ΔC), which functions to uncouple Gα13 from GPCR (Shan et al., 2006), or secondary to expression of Gα13 truncation mutant lacking amino acids from 255V-260R (Gα13-Δ255-260), which cannot associate with the Gα13 effector p115RhoGEF and thereby does not induce RhoA activation (unpublished data; Meigs et al., 2005). These findings together show the key function of Gα13 interaction with VE-cadherin in inducing VE-cadherin internalization in a GPCR- and RhoA-independent manner.

Second messenger H_2O_2 induces Gα13/Src interaction and Src activation

Because the Src kinase inhibitor PP1 prevented the Gα13-mediated AJ disruption (Fig. 1 O and unpublished data), we next addressed the possible role of Src in mediating the loss of endothelial barrier function induced by the aforementioned interaction of Gα13 with VE-cadherin. Src may be important in this context because Src-dependent phosphorylation of VE-cadherin at Tyr 658 was shown to uncouple p120-catenin from VE-cadherin leading to the internalization of VE-cadherin (Potter et al., 2005; Hatanaka et al., 2011; Orsenigo et al., 2012). In these studies, we challenged HMVEC-L with H_2O_2, the common and relatively long-lived ROS known to be generated in response to multiple inflammatory mediators (Rhee, 2006). We observed that H_2O_2 induced Src phosphorylation at Tyr 416 as well as VE-cadherin phosphorylation at

Tyr 658 (Fig. 2 A and not depicted). The H_2O_2–dependent phosphorylation of both proteins, however, was significantly reduced after Gα13 depletion (Fig. 2 A). Phosphorylation of bacterially expressed GST-tagged VE-cadherin cytoplasmic domain (CD) at Tyr 658 by Src was increased by functional Gα13/i chimeras (Chen et al., 2005) in the presence of either GTP-γS or AlF_4^- (Fig. 2 B), demonstrating that Src activation in the presence of GTP-bound Gα13 could thereby induce Src phosphorylation of VE-cadherin.

That Src formed a complex with Gα13 was evident from the findings that Gα13 coimmunoprecipitated with several Src family proteins c-Src, Fyn, Lyn-A, and c-Yes (Fig. 2 C). These interactions required the Src kinase domain (aa 244–541), as well as Gα13 switch region II-III (aa 213–265; Fig. 2, D and E). Consistent with our model, the interaction of Src was enhanced by expression of the constitutively active Gα13 Q226L mutant (Fig. 2, D and E).

Gα13-mediated Src activation induces endothelial permeability by dissociating p120-catenin from VE-cadherin

Overexpression of Gα13 in HMVEC-L induced VE-cadherin phosphorylation at Tyr 658 (unpublished data), and prevented the binding of p120-catenin to VE-cadherin (Fig. 3 A). Challenging Gα13-depleted HMVEC-L with TNF, in contrast, prevented p120-catenin dissociation from VE-cadherin (Fig. 3 B), further supporting our concept that Gα13 plays key role in mediating Src activation, the dissociation of p120-catenin from VE-cadherin, and the endothelial permeability response. The importance of Tyr 658 on VE-cadherin for p120-catenin binding was shown functionally by measuring endothelial barrier integrity and VE-cadherin internalization. Endothelial integrity was lost by depletion of VE-cadherin in HMVEC-L but was restored by expression of WT mouse VE-cadherin and, importantly, by expressing the phosphorylation-resistant Y658F
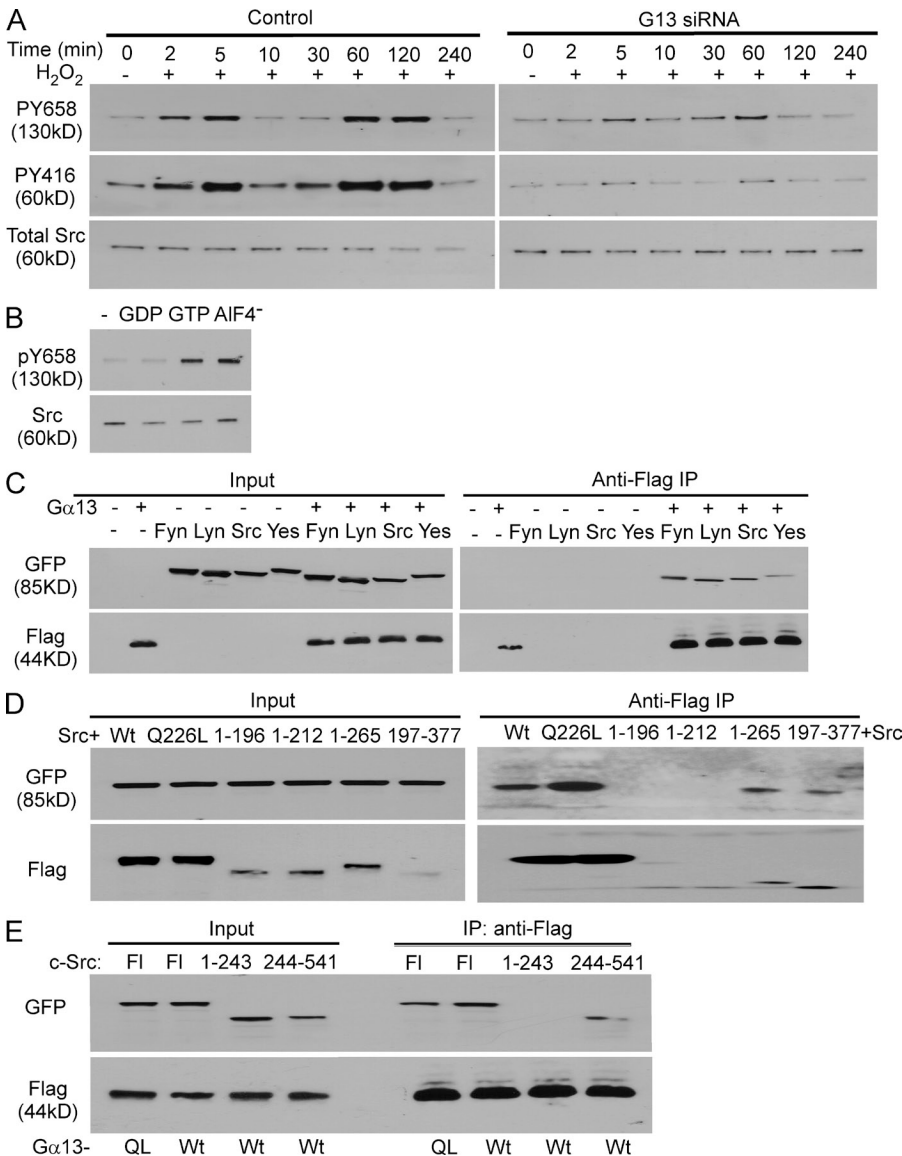

Figure 2. Gα13 signaling induces Src activation and VE-cadherin phosphorylation. (A) HMVEC-L cells were infected with control or Gα13 siRNA lentivirus, and treated with 300 μM H_2O_2. Src activation was determined by Tyr 416 phosphorylation and VE-cadherin phosphorylation at Tyr 658 was analyzed by WB. The experiment was performed twice with similar results. (B) Purified GST-tagged VE-cadherin-CD expressed by bacterial was incubated with Src prepared by immunoprecipitation from confluent HMVEC-L cells in the presence of purified Gα13/i chimeras with 10 μM GDP or GTPγS or 30 μM AlF_4^-. Phosphorylation of purified VE-cadherin-CD at Tyr 658 was assessed by WB. Results are representative of three experiments. (C) 293T cells were transfected with plasmids encoding Flag-tagged Gα13 or GFP-tagged Src family members Fyn, Lyn, c-Src, and c-Yes. Lysates were precipitated with anti-Flag antibody, and immunoprecipitates were detected by WB using anti-Flag and anti-GFP antibodies. Results are representative of two experiments. (D) 293T cells were co-transfected with plasmids encoding GFP-tagged Src with Flag-tagged Wt-Gα13, Q226L-Gα13, or Gα13 truncation mutants. Cell lysates were precipitated with anti-Flag antibody, and immunoprecipitates were detected by WB using anti-Flag and anti-GFP antibodies. Results are representative of two experiments. (E) 293T cells were co-transfected with plasmids encoding Flag-tagged Wt-Gα13 or Q226L-Gα13, with truncation mutants of GFP-tagged c-Src. Cell lysates were precipitated with anti-Flag antibody, and immunoprecipitates were detected by WB using anti-Flag and anti-GFP antibodies. Results are representative of two experiments.

VE-cadherin mutant (Fig. 3, C and D). The expression of phosphorylation mimic Y658E VE-cadherin mutant promoted VE-cadherin internalization, and thus only partially restored endothelial permeability (Fig. 3, C and D). Expression of Y658F VE-cadherin mutant also prevented endothelial barrier disruption induced by TNF (Fig. 3 E). Together, these findings demonstrate the essential role of Tyr658 on VE-cadherin in the mechanism of VE-cadherin internalization and subsequent endothelial barrier disruption.

H_2O_2 signaling of Src activation is required for VE–cadherin internalization

To interrogate whether Src activation occurring downstream of Gα13 signaling mediated VE-cadherin internalization, we focused on the role of H_2O_2, the oxidant recognized as a crucial second messenger mediating dissociation of several G proteins, Gαi, Gαo, and Gα12, from their respective GPCRs (Nishida et al., 2000; Yu et al., 2012). We observed that a diverse set of inflammatory mediators known to increase endothelial permeability (VEGF, LPS, and TNF) induced the production of H_2O_2 in endothelial cells (Fig. 4 A). This likely occurred through activation of the oxidase Nox2 induced by these mediators (Diebold et al., 2009; Li et al., 2009; Clement et al., 2010). H_2O_2 also activated Gα13 (Fig. 4 B) in a dose-dependent manner, as determined by the trypsin sensitivity assay (Nishida et al., 2000). In addition, H_2O_2 itself (Fig. 4 C) or H_2O_2 generated by VEGF (Fig. 4 D) induced the interaction of Gα13 with Src. These responses were sensitive to
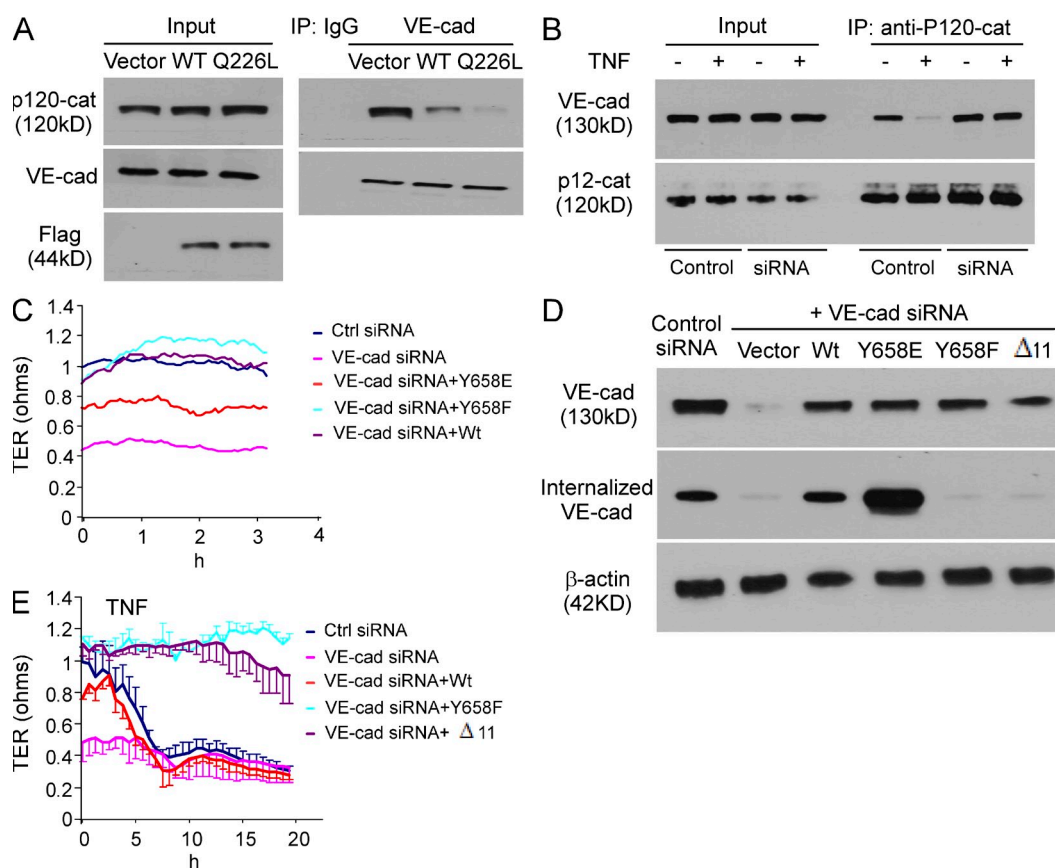

Figure 3.   Gα13 binding mediates p120–catenin dissociation from VE–cadherin through Src–dependent VE–cadherin phosphorylation at Tyr 658. (A) HMVEC-L cells were infected with lentivirus expression WT or Q226L Gα13. Cell lysates were precipitated with anti–p120-catenin antibody. Immunoprecipitates were detected by WB using anti-Flag, anti-p120-catenin, and anti–VE-cadherin antibodies. Results are representative of two experiments. (B) Confluent HMVEC-L cells infected with control or Gα13 siRNA lentivirus were stimulated with TNF. Cell lysates were precipitated by anti–p120-catenin antibody. Immunoprecipitates were detected by WB using anti–VE-cadherin and anti–p120-catenin antibodies. Results are representative of two experiments. (C) Confluent HMVEC-L cells infected with lentivirus encoding WT, Y658E, or Y658F mouse VE-cadherin were transfected with VE-cadherin siRNA oligonucleotides to deplete human VE-cadherin expression, and subjected to TER assay to measure endothelial junctional barrier integrity. TER values of each monolayer were normalized to values of control siRNA-treated cells at basal level. Data are expressed as mean ± SD (n = 3–4 in each group). Data are representative of two experiments and expressed as mean value (n = 3–4 in each group). (D) HMVEC-L cells infected with lentivirus encoding WT mouse VE-cadherin, as well as Y658E, Y658F, or Δ11 mutants were then transfected with siRNA oligonucleotides targeting human VE-cadherin. Expression and internalization of VE-cadherin in these cells were detected by WB. Results are representative of three experiments. (E) Cells used in D were also stimulated with TNF and subjected to TER assay to measure AJ integrity. Data are expressed as mean ± SD (n = 3–4 in each group). The experiments were performed twice with similar results.

the broad ROS scavenger *N*-acetyl-L-cysteine (NAC) and the NOX inhibitor diphenyleneiodonium (DPI; Fig. 4, C and D). Together, these findings showed that inflammatory mediator–generated H_2O_2 resulting in Src activation and subsequent phosphorylation of VE-cadherin is a key determinant of Gα13-mediated VE-cadherin internalization.

Identification of site of Gα13–VE-cadherin interaction responsible for disruption of AJs

We observed that the interaction between VE-cadherin and Gα13 was significantly enhanced by AlF_4^- (Fig. 5, A–C), GTPγS loading (Fig. 5, B and C), and H_2O_2 itself (Fig. 5 D) used to

activate Gα13 in vivo in endothelial cells or in vitro using purified Gα13/i chimeras (Chen et al., 2005) and GST-tagged VE-cadherin CD (Fig. 5 B). Gα13–VE-cadherin interaction increased in a ROS- and time-dependent manner in response to oxidative stress induced by H_2O_2 or VEGF (Fig. 5, D and E). Thus, oxidant activation of Gα13 resulting in GTP binding to Gα13 was responsible for Gα13 binding to VE-cadherin.

To identify binding motifs on Gα13 and VE-cadherin responsible for this interaction, we incubated 293T cell lysates containing Flag-tagged WT Gα13 and truncation mutants with purified GST-tagged full-length VE-cadherin CD and truncation mutants. Full-length Gα13 and truncation mutants 1–212,
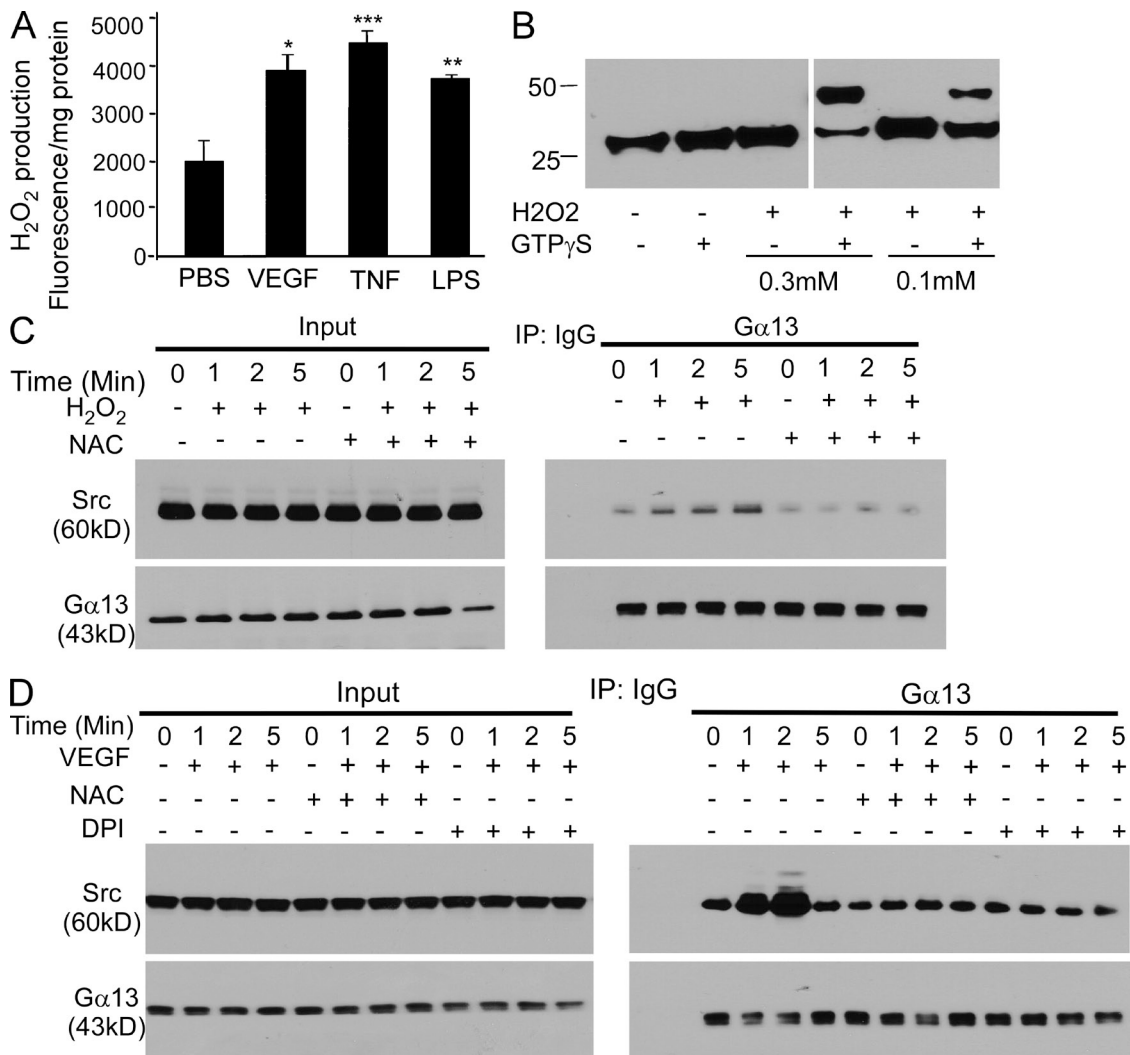

Figure 4. **H_2O_2 induces Gα13 activation and interaction of Gα13 with Src.** (A) Confluent HMVEC-L cells were stimulated by multiple inflammatory mediators and H_2O_2 production was assessed 1 h later. Mean ± SD (*n* = 3 in each group). Results are representative of two experiments. (B) HMVEC-L cell membrane fraction was extracted by CHAPS buffer and treated with trypsin in the presence of varying concentration of H_2O_2 and 50 µM GTP-γS. GTP-γS–loaded Gα13 was protected from digestion by trypsin. Results are representative of two experiments. (C) Serum-starved HMVEC-L cells were treated by 10 mM of the general ROS scavenger NAC for 30 min, and then challenged by 100 µM H_2O_2 at different times. Cell lysates were immunoprecipitated by control IgG or anti-Gα13 antibody, and immunoprecipitates were blotted with antibodies against Gα13 and Src. Results are representative of two experiments. (D) Serum-starved HMVEC-L cells were treated by 10 mM ROS scavenger NAC or 100 µM of the general NOX inhibitor DPI for 30 min, and then stimulated with 20 ng/ml VEGF at different times. Cell lysates were immunoprecipitated by control IgG or anti-Gα13 antibody, and immunoprecipitates were blotted with antibodies against Gα13 and Src. Results are representative of two experiments.
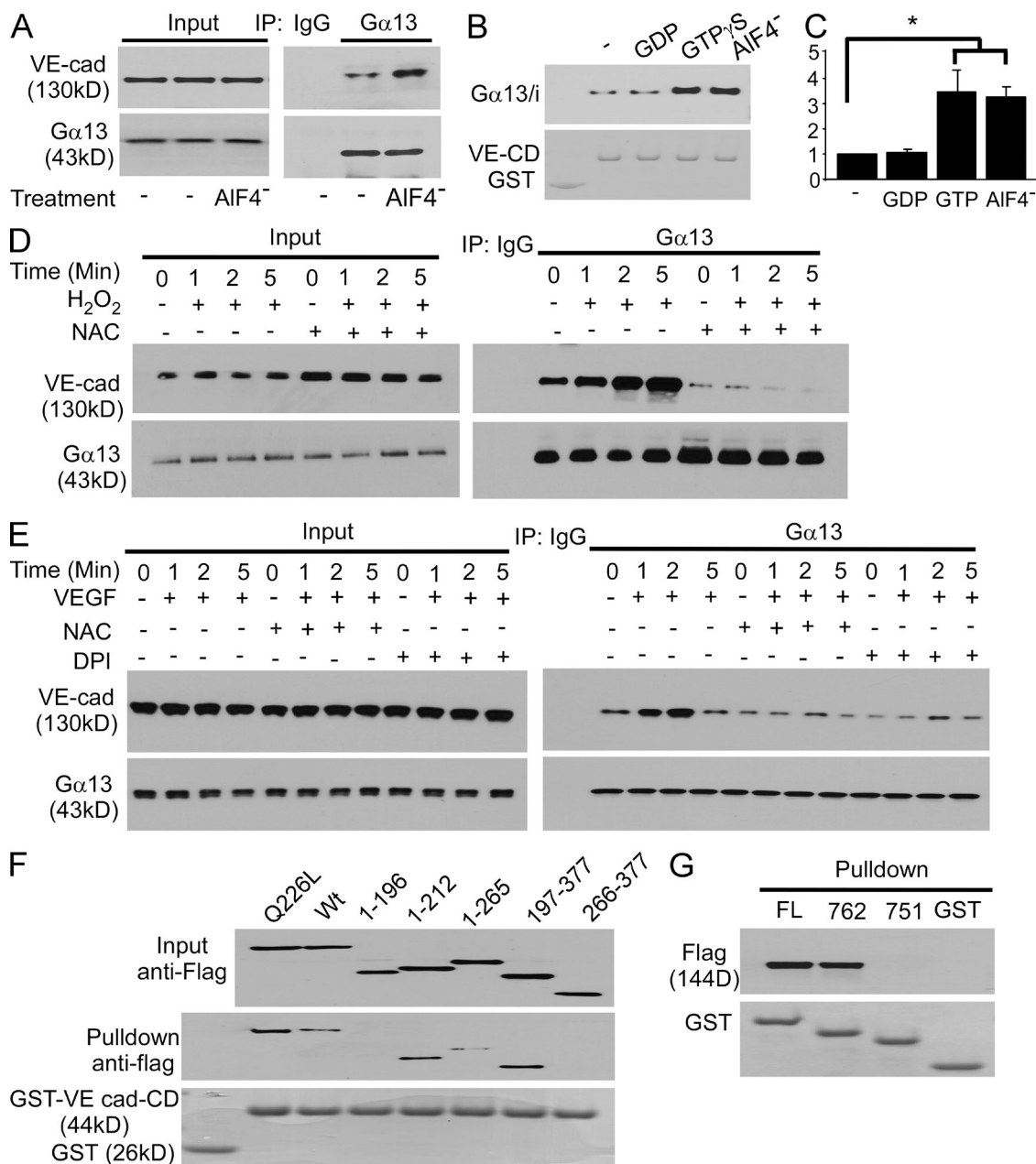
Figure 5. Gα13 binding to VE-cadherin in response to inflammatory mediators. (A) Confluent HMVEC-L cells were lysed in modified RIPA buffer and immunoprecipitated by control IgG or anti-Gα13 antibody with or without 30 µg AlF₄⁻. Immunoprecipitates were blotted with anti-bodies against Gα13 and VE-cadherin. Results are representative of two experiments. (B) GST-tagged VE-cadherin CD bound to glutathione beads and 6His-tagged Gα13/i chimeras were purified from bacteria, mixed with each other in the presence of 10 µM GDP, 10 µM GTP-γS, or 30 µM AlF₄⁻. The bound proteins were immunoblotted with antibody to 6His tag. The experiment was performed three times with similar results. (C) Quantification of (B; mean ± SD) from three experiments. *, P < 0.005. (D) Serum-starved HMVEC-L cells were treated with 10 mM of NAC for 30 min, stimulated by 100 µM H₂O₂ for different periods, solubilized, and subjected to VE-cadherin immunoprecipitation with anti-Gα13 antibody. Results are representative of two experiments. (E) Serum-starved HMVEC-L cells were treated by 10 mM of NAC or 100 µM DPI for 30 min, stimu-lated by 20 ng/ml of VEGF for different periods, solubilized, and subjected for VE-cadherin immunoprecipitation with anti-Gα13 antibody. Results are representative of two experiments. (F) 293T cells were transfected with Flag-tagged WT Gα13 and truncation mutants. Lysates were precipi-tated with GST- or GST-VE-cadherin CD-bound glutathione beads. Bead-bound proteins were immunoblotted with anti-Flag antibody. Results are representative of two experiments. (G) 293T cells were transfected with Flag-tagged WT Gα13. Cell lysates were incubated with GST- or GST-VE-cadherin CD truncation mutant-bound glutathione beads. Bead-bound proteins were immunoblotted with anti-Flag antibody. Results are representative of two experiments.
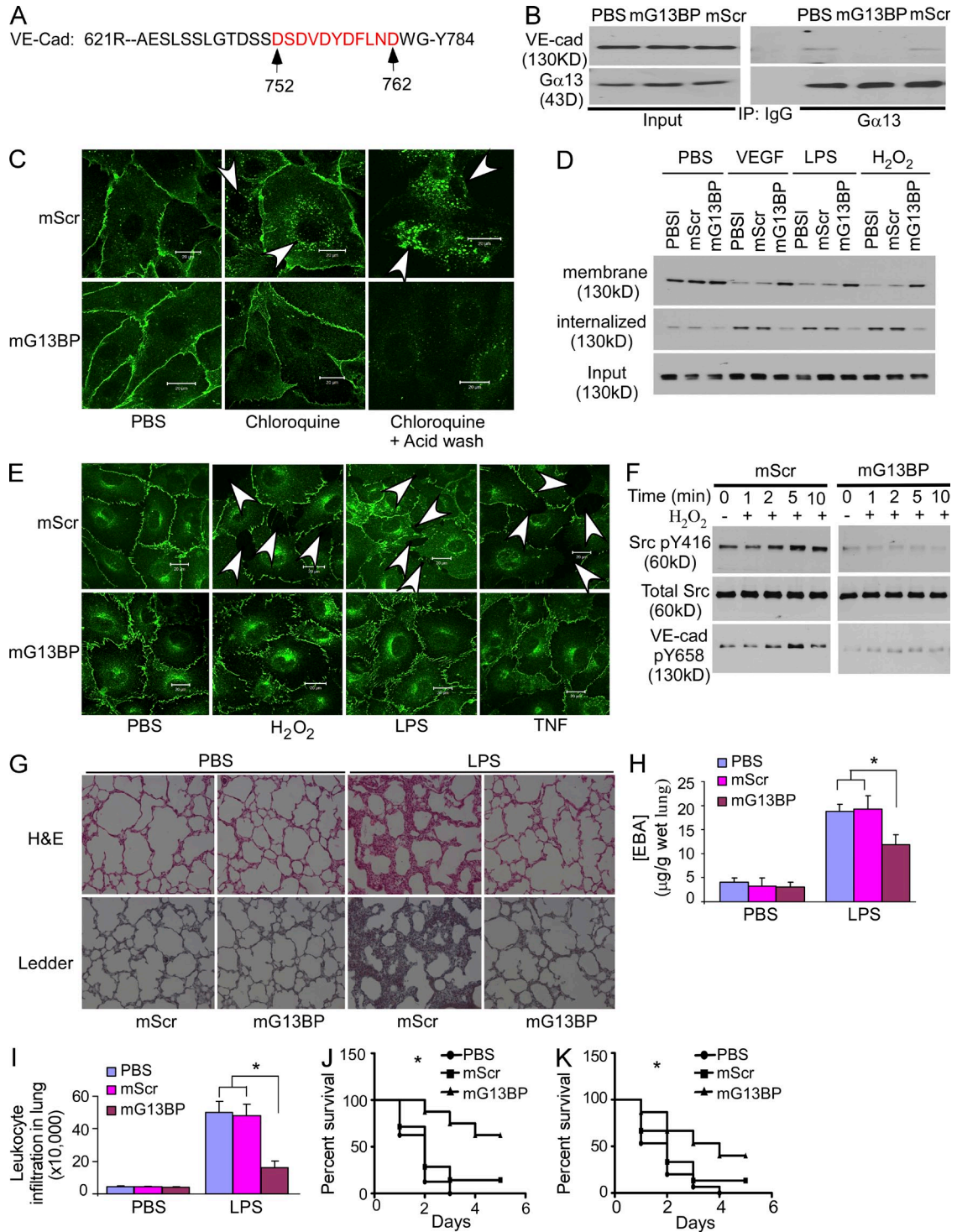
Figure 6. mG13BP prevents endothelial barrier disruption through blocking the interaction of Gα13 with VE-cadherin. (A) Human VE-cadherin cytoplasmic domain sequence. The Gα13 binding motif is highlighted in red. (B) HMVEC-L cells were lysed in modified RIPA buffer. Cell lysates were immunoprecipitated with anti-Gα13 antibody in the presence of 200 mM mScr or mG13BP. Immunoprecipitates were immunoblotted with antibody to Gα13 or VE-cadherin. Figures are representative of three experiments. (C) Confocal microscopy images of VE-cadherin subcellular location in mScr- or mG13BP-pretreated HMVEC-L cells in the presence or absence of chloroquine for 3 h. Green indicates VE-cadherin. Arrows point to internalized VE-cadherin. Figures are representative of two experiments. Bars, 20 μM. (D) Serum-starved confluent HMVEC-L cells were pretreated with PBS, 150 μM mScr, or mG13BP for 30 min, and then stimulated by 20 ng/ml VEGF, 2 μg/ml LPS, or 100 μM H$_2$O$_2$ and subjected to biotinylation. Cells were then incubated at either 4°C to block membrane trafficking or 37°C to allow internalization. Purified biotinylated proteins were then assessed by WB using anti-VE-cadherin antibody. The experiment was performed twice with similar results. (E) Confluent HMVEC-L cells were pretreated with PBS, 150 μM mScr, or 150 μM mG13BP, and then stimulated with PBS, 300 μM H$_2$O$_2$, 2 μg/ml LPS, or

197–265, and 197–377 bound to VE-cadherin CD, and the binding was increased by the constitutively active Gα13 mutant Q226L (Fig. 5 F); thus, Gα13 switch region I motif from amino acids 197–212 was essential for Gα13 binding to VE-cadherin. Interestingly, this motif is also required for Gα13 interaction with other established Gα13 effectors, integrins, p115RhoGEF, and E-cadherin (Meigs et al., 2005; Gong et al., 2010). We observed that Gα13 associated with the full-length VE-cad-CD and C-terminal truncation mutant Δ762, but not with Δ751 (Fig. 5 G), indicating that this highly conserved (Kaplan et al., 2001) negatively charged 11-aa motif within VE-cad-CD (Fig. 6 A) was essential for Gα13 binding.

Peptide mG13BP prevents Gα13 binding to VE-cadherin and endothelial barrier dysfunction

To address the functional significance of the identified 11-aa VE-cadherin motif, we studied Gα13–VE-cadherin interaction in the presence of the myristoylated Gα13-binding peptide (mG13BP) of VE-cadherin, Myr-DSDVDYDFLND, corresponding to VE-cadherin-CD aa 752–762 (Fig. 6 A). This cell permeable peptide prevented the binding of Gα13 to VE-cadherin (Fig. 6 B), as well as VE-cadherin internalization in the presence of multiple tested inflammatory mediators VEGF, LPS, and H_2O_2 (Fig. 6, C and D). Expression of VE-cadherin truncation mutant lacking Gα13 binding motif (VE-cad-Δ11) in endothelial cells also prevented VE-cadherin internalization (Fig. 3 D) and AJ disruption induced by TNF (Fig. 3 E), further supporting the critically important role of Gα13 binding to VE-cadherin in regulating endothelial permeability.

Treatment of endothelial monolayers with mG13BP significantly reduced AJ disassembly and endothelial permeability in response to multiple inflammatory mediators (Fig. 6 E). In addition, treatment of endothelial cells with mG13BP prevented oxidative stress–induced Src activation and Src-dependent VE-cadherin phosphorylation at Tyr 658 (Fig. 6 F), suggesting that Gα13/VE-cadherin interaction was responsible for the aforementioned Src activation.

To address potential in vivo antiinflammatory function of mG13BP peptide, which prevented Gα13/VE-cadherin interaction (Fig. 6 B), we challenged mice with LPS. When mice showed signs of lung injury, they were treated with mG13BP. We observed that mG13BP inhibited leukocyte transmigration and transvascular permeability of Evans blue albumin tracer in response to LPS (Fig. 6, G–I). Moreover, mG13BP significantly enhanced survival in both LPS and CLP mouse sepsis models relative to controls (Fig. 6, J–K).

DISCUSSION

We have identified here a unique proinflammatory function of a previously unknown interaction of the GTP-bound Gα13 subunit with VE-cadherin in mediating the disassembly of endothelial AJs, and thereby the disruption of the endothelial barrier. This interaction occurred in response to the relatively long-lived oxidant H_2O_2 (Kress et al., 1995; Giniatullin and Giniatullin, 2003) that is generated in endothelial cells by a variety of inflammatory mediators, including LPS, TNF, and VEGF (Frey et al., 2009). In each instance, H_2O_2 generation is known to be secondary to activation of Nox2 (Frey et al., 2009; Gandhirajan et al., 2013). That the global ROS scavenger NAC (Shimizu et al., 2004; Bauernfeind et al., 2011) and Nox inhibitor DPI (Wind et al., 2010; Bauernfeind et al., 2011) prevented the binding of Gα13 with VE-cadherin supported our contention that AJ disassembly and permeability responses were initiated by ROS production induced by the inflammatory mediators. We did not specifically address the effects of H_2O_2 generation. It is well established that superoxide and H_2O_2 are the primary oxidants produced in endothelial cells that can disrupt endothelial barrier function (Cai, 2005) and also that H_2O_2 is the primary oxidant species generated because the high levels of expression of superoxide dismutases in endothelial cells efficiently convert superoxide to H_2O_2 (Fridovich, 1995; Cai, 2005). We observed that the interaction of Gα13 with VE-cadherin secondary to ROS occurred independently of GPCR activation because none of mediators tested are known to directly activate GPCRs (Shi et al., 2004; Khoa et al., 2006; Shan et al., 2006). We also observed that expression of the Gα13 ΔC mutant unable to bind to GPCRs (Shan et al., 2006) was itself capable of activating Src and inducing VE-cadherin internalization, an event that preceded AJ disassembly. Our concept that the α subunit of heterotrimeric G proteins functions independently

20 ng/ml TNF, and analyzed by immunostaining using anti–VE-cadherin antibody. Figures are representative of three experiments. Bars, 20 μM. (F) Confluent HMVEC-L cells were pretreated with PBS, 150 μM mScr, or 150 μM mG13BP, and then stimulated with 300 μM H_2O_2. Src activation and VE-cadherin phosphorylation on Tyr 658 were assessed by WB using indicated antibodies. Figures are representative of three experiments. (G) C57/BL6 mice were first challenged by 20 mg/kg LPS i.p., and then received 2 mg/kg mScr or mG13BP 30 min by retroorbital venous injection. Mouse lungs were fixed by 10% formalin, dissected, and subjected to H&E and Ledder staining. Studies were made with n = 3 mice in each group from 2 experiments. (H) C57/BL6 mice were i.p. injected with PBS or 20 mg/kg LPS, and then 30 min later received PBS, 2 mg/kg mScr, or mG13BP. Evans blue tracer (40 mg/kg) was given at indicated time points. Mouse lungs were harvested 30 min after Evans blue dye injection and transvascular albumin permeability was measured. Mean ± SD; studies were made with n = 4 in each of the 3 PBS and 3 LPS group. *, P < 0.01. Figures are representative of two experiments. (I) C57BL6 mice were given 20 mg/ml LPS i.p., and then treated with 2 mg/kg mG13BP, mScr, or vehicle PBS by injection through retroorbital vein given 2 h after LPS. Leukocytes in lung bronchoalveolar lavage (BAL) 24 h after LPS challenge were centrifuged and counted. Studies were made with n = 4 in each of 3 PBS and 3 LPS groups. *, P < 0.01. Figures are representative from two experiments. (J) C57/BL6 mice were challenged with 40 mg/kg LPS i.p., and then received PBS, 2 mg/kg mScr, or mG13BP by retroorbital venous injection 30 min after LPS, and survival was monitored. Studies were made with n = 8 in each of the 3 groups. Figures are representative from two experiments. (K) C57/BL 6 mice were subjected to CLP to induce polymicrobial sepsis. At 30 min after surgery, mice received PBS, 2 mg/kg mScr, or mG13BP by retroorbital injection, and survival was monitored. Differences in mortality were assessed by log-rank test. Studies were made with n = 15 in each of the three groups. *, P < 0.05. Figures are representative from two experiments.

of GPCR activation is consistent with studies showing that ROS induce dissociation of the α subunit from heterotrimeric G proteins independent of GPCR ligation with agonists (Nishida et al., 2000; Yu et al., 2012). We observed that Gα13 binding to VE-cadherin in turn induced Src activation, and thereby the internalization of VE-cadherin. This effect triggered by Gα13 binding to VE-cadherin appeared to be independent of RhoA because Gα13 truncation mutant Δ255-260 lacking the p115RhoGEF binding motif (corresponding to the Gα12 Δ244-249 mutant; Meigs et al., 2005) was itself able to induce the Src activation and phosphorylation of VE-cadherin at Tyr 658 required for VE-cadherin internalization (Xiao et al., 2003; Potter et al., 2005; Hatanaka et al., 2011).

An important observation in these studies is the finding that disruption of AJs induced by the activated Gα13 was rescued by Src kinase inhibition. Exposing endothelial cells to H_2O_2 induced Src phosphorylation at Tyr 416, a defining signature of Src activation (Roskoski, 2005). The mechanism of Src activation may be through H_2O_2-mediated inhibition of protein tyrosine phosphatase (Salmeen and Barford, 2005; Su et al., 2012), as well as direct H_2O_2–dependent oxidation of Src (Giannoni et al., 2005). In this study, we demonstrated that Src activation in endothelial cells required H_2O_2 generation induced by the inflammatory mediators and was facilitated by the Gα13/VE-cadherin interaction. Src activation in turn mediated phosphorylation of VE-cadherin at Tyr 658, the phosphorylation site known to promote the dissociation of p120-catenin from VE-cadherin and the subsequent internalization of VE-cadherin (Xiao et al., 2003; Potter et al., 2005; Hatanaka et al., 2011). Although the role of Src and resulting VE-cadherin phosphorylation at Tyr658 in mediating disassembly of AJs has been previously proposed (Adam et al., 2010), our results are the first to show that in the context of Src activation induced by Gα13–VE-cadherin interaction, Src phosphorylation of VE-cadherin at Tyr656 is an important mechanism of AJ disassembly. This contention is reinforced by the finding that endothelial cell expression of phosphorylation-resistant Y658F VE-cadherin not only restored endothelial AJ integrity but also protected AJs from disruption induced by multiple inflammatory mediators. The signaling function of H_2O_2 generated by the mediators tested induced both the interaction of Gα13 with VE-cadherin, and thus the Src activation responsible for VE-cadherin internalization.

We pinpointed the domain on active Gα13 required for the binding to Src and VE-cadherin. Gα13 immunoprecipitated with several Src family kinases (c-Src, Fyn, Lyn-A, and c-Yes). This interaction was dependent on the Src kinase domain (aa 244–541) and the switch region II-III (aa 213–265) of Gα13. Gα13 switch region I motif from aa 197–212 was also essential for Gα13 binding to VE-cadherin. It appears from these results that VE-cadherin serves as a scaffold for binding both Src and Gα13 after H_2O_2 generation, but they bind to different sites on VE-cadherin. Interestingly, it is known that the switch region I motif on Gα13 is the same domain required for Gα13 interaction with other known effectors, such as integrins and E-cadherin (Meigs et al., 2005; Gong et al., 2010).

We observed that Gα13 associated with the VE-cadherin C-terminal truncation mutant Δ762 but not with Δ751, indicating that this highly conserved (Meigs et al., 2002) negatively charged 11-aa motif DSDVDYDFLND (termed mG13BP) was responsible for VE-cadherin interaction with Gα13. This result was supported by the finding that endothelial cells expressing the VE-cadherin truncation mutant lacking the 11 aa were resistant to TNF-induced permeability response because of diminished VE-cadherin internalization.

We studied the possible therapeutic significance of the 11-aa peptide in mice by myristoylating the peptide to enable its cell penetration. In endothelial cells, mG13BP prevented the binding of Gα13 to VE-cadherin and internalization of VE-cadherin and significantly reduced AJ disassembly and endothelial permeability in response to proinflammatory mediators. In mice, mG13BP reversed the increased lung vascular permeability and leukocyte transmigration responses and also significantly enhanced survival in mouse models of sepsis.

In conclusion, our studies describe a novel function of binding of active Gα13 to VE-cadherin in activating AJ disassembly and increasing endothelial permeability in response to multiple proinflammatory mediators. These studies have uncovered a common mechanism of endothelial barrier disruption and inflammation functioning through the generation of H_2O_2 that resulted in the interaction of Gα13 subunit and Src with VE-cadherin. Src, in turn, phosphorylated VE-cadherin at Tyr 658 and mediated disassembly of AJs through VE-cadherin internalization. A peptide used to prevent Gα13–VE-cadherin interaction (DSDVDYDFLND) abrogated the vascular permeability and inflammation responses in mouse models in sepsis. Thus, Gα13–VE-cadherin interaction represents a potential antiinflammatory target to prevent endothelial barrier disruption and vascular inflammation.

MATERIALS AND METHODS

Reagents. Myristoylated G13BP and scrambled peptide were synthesized and purified at the Research Resource Center at University of Illinois, Chicago. Anti-Gα13 (sc-410), anti-Src (sc-18, sc-5266), and anti–VE-cadherin (sc-9989 and sc-6458) antibodies, as well as human VE-cadherin siRNA were purchased from Santa Cruz Biotechnology; mouse monoclonal anti-Gα13antibody (26004) was from Neweast Biosciences; anti–phospho-Src Y416 antibody was obtained from Cell Signaling Technology; anti–phospho-VE-cadherin Y658 antibody, Src kinase assay kit, and anti–v-Src antibody were obtained from Millipore; anti–β-actin and anti-Flag (M2) antibodies, TNF, GDT and GTPγS, NAC, and DPI were purchased from Sigma-Aldrich; Lipofectamine 2000, anti-GFP antibody, and Lipofectamine 2000 were purchased from Invitrogen; HMVEC-L and Amaxa Nucleofector kit (VPB-1002) were obtained from Lonza; and HisPur Ni-NTA Spin Purification kit was obtained from Pierce. SensoLyte ADHP Hydrogen Peroxide Assay kit was from purchased AnaSpec. Anti-RhoA antibody and GST-Rhotekin beads were purchased from Cytoskeleton Inc.

Plasmid constructs. Mouse VE-cadherin full-length cDNA plasmid was purchased from Open Biosystems. Human VE-cadherin cDNA was prepared by RT-PCR. Y658E, Y658F, and Δ11 truncation mutant were made by overlapping PCR and inserted into pLVX-IRES-mcherry lentivirus vector. Gα13 plasmid was a gift from J. Profirovic (St. Louis College of Pharmacy, St. Luois, MO). Truncation mutants and Q226L point mutant were prepared by overlapping-PCR and inserted into pEF6-HisB or pLVX-IRES-mcherry

vectors. The small hairpin Gα12 and Gα13 siRNAs were inserted into pLL3.7 lentivirus vector.

Generation of endothelial cell–specific Gα13-deficient mice. The animal experiments were approved by the Animal Care Committee and Institutional Biosafety Committee of the University of Illinois, Chicago. For in vivo experiments, we used endothelial cell–specific Gα13-deficient mice generated by i.p. tamoxifen 2 mg/d for 5 d into Tie2-Cre Gna13$^{flox/flox}$ mice (129/B6 background), in which tamoxifen induced expression of a fusion protein of Cre recombinase with the modified estrogen receptor binding domain (Cre ER^{T2}) under the control of the tie2 promoter (Indra et al., 1999; Korhonen et al., 2009). Gna13$^{flox/flox}$ mice were generated by backcrossing tie2-cre recombinase transgenic Gna12$^{-/-}$ and Gna13$^{flox/flox}$ alleles (S. Offermanns, Max-Planck Institute for Heart and Lung Research, Bad Nauheim, Germany) with 129/B6 mice. Experiments were performed at day14 from the first day of injection (Korhonen et al., 2009).

Coimmunoprecipitation and in vitro binding assays. These assays were performed as reported with minor modifications (Gong et al., 2010). For coimmunoprecipitation experiments, endothelial cell lysates were incubated with either a rabbit anti-Gα13 antibody or an equal amount of normal rabbit IgG and, subsequently, with protein A/G-conjugated Sepharose beads, and then analyzed by Western blotting. In some experiments, 200 μM mG13BP or mScr control peptide was incubated with cell lysates before immunoprecipitation. For in vitro binding experiments, purified functional 6His-tagged Gα13/i chimeras or 293T cell lysate containing Flag-tagged Gα13 truncation mutants were added to agarose beads conjugated with GST or GST-tagged VE-cadherin-CD and truncation mutants in the presence or absence of 10 μM GDP, 10 μM GTPγS, or 30 μM AlF$_4$$^-$.

Transendothelial electrical resistance measurement. Serum-starved confluent endothelial cells plated on gold microelectrodes were infected with Gα13 siRNA lentivirus, or pretreated with 150 μM mG13BP or mScr control peptide, and challenged with 20 ng/ml VEGF, 2 μg/ml LPS, 20 ng/ml TNF, or 300 μM H$_2$O$_2$. TER was monitored using the ECIS system (Applied Biophysics) as previously described (Mirza et al., 2010).

Evans blue albumin pulmonary transvascular flux measurement. 24 h after 20 mg/kg LPS i.p., 40 mg/kg Evans blue albumin was retroorbitally injected into LPS-challenged WT and Gα13 CKO mice, or C57BL/6 mice received peptide 30 min after LPS challenge. Intravascular Evans blue was washed by PBS perfusion from right ventricle for 5 min. Mouse lungs were excised, weighed, homogenized in 1 ml PBS, and extracted in 2 ml formamide for 24 h at 60°C. Evans blue content was determined by OD620 and OD740 of the formamide extract (Vandenbroucke St Amant et al., 2012).

In vivo mG13BP peptide treatment protocol. Control scrambled mScr peptide and mG13BP was dissolved in PBS to make the stock solution of 0.5 mg/ml. For in vivo experiments, 2 mg/kg peptide or equal volume of PBS was injected via retroorbital vein.

Cell surface biotinylation and endocytosis assays. Serum starved monolayer HMVEC-Ls were washed twice with ice-cold HBSS with 1 mM calcium, and then incubated with 0.5 mg/ml of NHS-SS-biotin for 30 min in 4°C. To determine cell surface VE-cadherin expression, labeled cells were lysed in modified RIPA buffer, precipitated with streptavidin-conjugated agarose beads, and subjected to WB with anti–VE-cadherin antibody (Wu et al., 2005). For VE-cadherin endocytosis assay, biotinylated cells were washed twice with HBSS. The noninternalized cell surface proteins were cleaved by 50 mM glutathione in HBSS at 4°C for 30 min (Wu et al., 2005). To visualize the internalization of VE-cadherin, living cells were labeled by BV9 (anti–VE-cadherin extracellular domain antibody) in the presence or absence of 100 μM chloroquine at 37°C for 3 h (Xiao et al., 2003), fixed, and subjected to mild acid buffer wash (2 mM PBS-glycine, pH 2.0, 2 min twice) to remove cell surface-bound antibody (Gavard et al., 2008), and detected by Carl Zeiss confocal microscope using MLS510 meta software.

Src kinase assay. Purified Gα13/i chimeras and GST-tagged VE-cadherin CD were incubated with Src immunoprecipitated from HMVEC-L in the kinase assay buffer with or without GTPγS and AlF$_4$$^-$. Src kinase activity was determined by the phosphorylation of VE-cadherin at Tyr 658.

Trypsin sensitivity assay. The cell membranes (50 mg protein per tube) from HMVEC-L were solubilized by 1% CHAPS in 50 mM Hepes, pH 7.4, and incubated in buffer containing 25 mM Hepes, pH 7.5, 1 mM EDTA, 20 mM 2-mercaptoethanol, 25 mM MgCl$_2$, 100 mM NaCl, 0.7% CHAPS, and 10 μM GDP with or without 50 μM GTP-γS in the absence or presence of different concentration of H$_2$O$_2$ for 30 min at 30°C. Samples were then digested by 100 mg/ml-1 N-tosyl-L-phenylamine chloromethyl ketone (TPCK)-trypsin (1:25 ratio of trypsin to total protein) for 15 min at room temperature. The different digestion patterns of Gα13 were detected by Western blotting.

RNA interference and lentivirus preparation. Lentivirus preparation and infection were performed as previously described (Gong et al., 2010). Gα13 siRNA target sequence was as follows: 5′-GCAACGTGATCAAAGGTAT-3′.

Sepsis models. 129/B6 background Gα13 CKO mice and same background Gna13$^{flox/flox}$ mice, as well as WT C57/BL6 mice, were challenged with CLP or LPS i.p. CLP-mediated polymicrobial sepsis was induced using a 16-gauge needle as in Bachmaier et al. (2007). For survival studies, mice were monitored 4 times daily for 5 d. For histology, paraffin-embedded tissue sections were stained with H&E or Ledder stain.

Endothelial cell H$_2$O$_2$ production. Monolayer of HMVEC-Ls were washed twice by PBS, and then incubated with Amplex red (80 μM) and horseradish peroxidase (10 mU/ml) for 30 min after VEGF, LPS, or TNF stimulation. Supernatants were carefully collected and fluorescence was measured in a multiplate reader (λex = 345 nm; λem = 595 nm). Cells were maintained at 37°C in HBSS buffer during the 30-min incubation time.

Quantification and statistics. Western blot bands were scanned and analyzed for uncalibrated optical density using National Institutes of Health Image J software. Student's t test and log-rank test were used to determine statistical significance with p-value set at <0.05.

REFERENCES

Adam, A.P., A.L. Sharenko, K. Pumiglia, and P.A. Vincent. 2010. Src-induced tyrosine phosphorylation of VE-cadherin is not sufficient to decrease barrier function of endothelial monolayers. *J. Biol. Chem.* 285:7045–7055. http://dx.doi.org/10.1074/jbc.M109.079277

Bachmaier, K., S. Toya, X. Gao, T. Triantafillou, S. Garrean, G.Y. Park, R.S. Frey, S. Vogel, R. Minshall, J.W. Christman, et al. 2007. E3 ubiquitin ligase Cblb regulates the acute inflammatory response underlying lung injury. *Nat. Med.* 13:920–926. http://dx.doi.org/10.1038/nm1607

Bauernfeind, F., E. Bartok, A. Rieger, L. Franchi, G. Núñez, and V. Hornung. 2011. Cutting edge: reactive oxygen species inhibitors block priming, but not activation, of the NLRP3 inflammasome. *J. Immunol.* 187:613–617. http://dx.doi.org/10.4049/jimmunol.1100613

Brown, J.H., D.P. Del Re, and M.A. Sussman. 2006. The Rac and Rho hall of fame: a decade of hypertrophic signaling hits. *Circ. Res.* 98:730–742. http://dx.doi.org/10.1161/01.RES.0000216039.75913.9e

Cai, H. 2005. Hydrogen peroxide regulation of endothelial function: origins, mechanisms, and consequences. *Cardiovasc. Res.* 68:26–36. http://dx.doi.org/10.1016/j.cardiores.2005.06.021

Chen, Z., W.D. Singer, P.C. Sternweis, and S.R. Sprang. 2005. Structure of the p115RhoGEF rgRGS domain-Galpha13/i1 chimera complex suggests convergent evolution of a GTPase activator. *Nat. Struct. Mol. Biol.* 12:191–197. http://dx.doi.org/10.1038/nsmb888

Chiasson, C.M., K.B. Wittich, P.A. Vincent, V. Faundez, and A.P. Kowalczyk. 2009. p120-catenin inhibits VE-cadherin internalization through a Rho-independent mechanism. *Mol. Biol. Cell.* 20:1970–1980. http://dx.doi.org/10.1091/mbc.E08-07-0735

Clement, H.W., J.F. Vazquez, O. Sommer, P. Heiser, H. Morawietz, U. Hopt, E. Schulz, and E. von Dobschütz. 2010. Lipopolysaccharide-induced radical formation in the striatum is abolished in Nox2 gp91phox-deficient mice. *J. Neural Transm.* 117:13–22. http://dx.doi.org/10.1007/s00702-009-0327-5

Cole, P.A., K. Shen, Y. Qiao, and D. Wang. 2003. Protein tyrosine kinases Src and Csk: a tail's tale. *Curr. Opin. Chem. Biol.* 7:580–585. http://dx.doi.org/10.1016/j.cbpa.2003.08.009

Correale, J., and A. Villa. 2007. The blood-brain-barrier in multiple sclerosis: functional roles and therapeutic targeting. *Autoimmunity.* 40:148–160. http://dx.doi.org/10.1080/08916930601183522

Dejana, E., F. Orsenigo, and M.G. Lampugnani. 2008. The role of adherens junctions and VE-cadherin in the control of vascular permeability. *J. Cell Sci.* 121:2115–2122. http://dx.doi.org/10.1242/jcs.017897

Diebold, I., T. Djordjevic, A. Petry, A. Hatzelmann, H. Tenor, J. Hess, and A. Görlach. 2009. Phosphodiesterase 2 mediates redox-sensitive endothelial cell proliferation and angiogenesis by thrombin via Rac1 and NADPH oxidase 2. *Circ. Res.* 104:1169–1177. http://dx.doi.org/10.1161/CIRCRESAHA.109.196592

Frey, R.S., M. Ushio-Fukai, and A.B. Malik. 2009. NADPH oxidase-dependent signaling in endothelial cells: role in physiology and pathophysiology. *Antioxid. Redox Signal.* 11:791–810. http://dx.doi.org/10.1089/ars.2008.2220

Fridovich, I. 1995. Superoxide radical and superoxide dismutases. *Annu. Rev. Biochem.* 64:97–112. http://dx.doi.org/10.1146/annurev.bi.64.070195.000525

Gandhirajan, R.K., S. Meng, H.C. Chandramoorthy, K. Mallilankaraman, S. Mancarella, H. Gao, R. Razmpour, X.F. Yang, S.R. Houser, J. Chen, et al. 2013. Blockade of NOX2 and STIM1 signaling limits lipopolysaccharide-induced vascular inflammation. *J. Clin. Invest.* 123:887–902.

Gavard, J., and J.S. Gutkind. 2006. VEGF controls endothelial-cell permeability by promoting the beta-arrestin-dependent endocytosis of VE-cadherin. *Nat. Cell Biol.* 8:1223–1234. http://dx.doi.org/10.1038/ncb1486

Gavard, J., V. Patel, and J.S. Gutkind. 2008. Angiopoietin-1 prevents VEGF-induced endothelial permeability by sequestering Src through mDia. *Dev. Cell.* 14:25–36. http://dx.doi.org/10.1016/j.devcel.2007.10.019

Giannoni, E., F. Buricchi, G. Raugei, G. Ramponi, and P. Chiarugi. 2005. Intracellular reactive oxygen species activate Src tyrosine kinase during cell adhesion and anchorage-dependent cell growth. *Mol. Cell. Biol.* 25:6391–6403. http://dx.doi.org/10.1128/MCB.25.15.6391-6403.2005

Giniatullin, A.R., and R.A. Giniatullin. 2003. Dual action of hydrogen peroxide on synaptic transmission at the frog neuromuscular junction. *J. Physiol.* 552:283–293. http://dx.doi.org/10.1113/jphysiol.2003.050690

Gong, H., B. Shen, P. Flevaris, C. Chow, S.C. Lam, T.A. Voyno-Yasenetskaya, T. Kozasa, and X. Du. 2010. G protein subunit Galpha13 binds to integrin alphaIIbbeta3 and mediates integrin "outside-in" signaling. *Science.* 327:340–343. http://dx.doi.org/10.1126/science.1174779

Hatanaka, K., M. Simons, and M. Murakami. 2011. Phosphorylation of VE-cadherin controls endothelial phenotypes via p120-catenin coupling and Rac1 activation. *Am. J. Physiol. Heart Circ. Physiol.* 300:H162–H172. http://dx.doi.org/10.1152/ajpheart.00650.2010

Holinstat, M., D. Mehta, T. Kozasa, R.D. Minshall, and A.B. Malik. 2003. Protein kinase Calpha-induced p115RhoGEF phosphorylation signals endothelial cytoskeletal rearrangement. *J. Biol. Chem.* 278:28793–28798. http://dx.doi.org/10.1074/jbc.M303900200

Huang, K., Y.H. Wang, A. Brown, and G. Sun. 2009. Identification of N-terminal lobe motifs that determine the kinase activity of the catalytic domains

and regulatory strategies of Src and Csk protein tyrosine kinases. *J. Mol. Biol.* 386:1066–1077. http://dx.doi.org/10.1016/j.jmb.2009.01.012

Indra, A.K., X. Warot, J. Brocard, J.M. Bornert, J.H. Xiao, P. Chambon, and D. Metzger. 1999. Temporal.controlled site-specific mutagenesis in the basal layer of the epidermis: comparison of the recombinase activity of the tamoxifen-inducible Cre-ER(T) and Cre-ER(T2) recombinases. *Nucleic Acids Res.* 27:4324–4327. http://dx.doi.org/10.1093/nar/27.22.4324

Kaplan, D.D., T.E. Meigs, and P.J. Casey. 2001. Distinct regions of the cadherin cytoplasmic domain are essential for functional interaction with Galpha 12 and beta-catenin. *J. Biol. Chem.* 276:44037–44043. http://dx.doi.org/10.1074/jbc.M106121200

Kelly, P., P.J. Casey, and T.E. Meigs. 2007. Biologic functions of the G12 subfamily of heterotrimeric g proteins: growth, migration, and metastasis. *Biochemistry.* 46:6677–6687. http://dx.doi.org/10.1021/bi700235f

Khoa, N.D., M. Postow, J. Danielsson, and B.N. Cronstein. 2006. Tumor necrosis factor-alpha prevents desensitization of Galphas-coupled receptors by regulating GRK2 association with the plasma membrane. *Mol. Pharmacol.* 69:1311–1319. http://dx.doi.org/10.1124/mol.105.016857

Kim, M.P., S.I. Park, S. Kopetz, and G.E. Gallick. 2009. Src family kinases as mediators of endothelial permeability: effects on inflammation and metastasis. *Cell Tissue Res.* 335:249–259. http://dx.doi.org/10.1007/s00441-008-0682-9

Klages, B., U. Brandt, M.I. Simon, G. Schultz, and S. Offermanns. 1999. Activation of G12/G13 results in shape change and Rho/Rho-kinase-mediated myosin light chain phosphorylation in mouse platelets. *J. Cell Biol.* 144:745–754. http://dx.doi.org/10.1083/jcb.144.4.745

Komarova, Y., and A.B. Malik. 2010. Regulation of endothelial permeability via paracellular and transcellular transport pathways. *Annu. Rev. Physiol.* 72:463–493. http://dx.doi.org/10.1146/annurev-physiol-021909-135833

Komarova, Y.A., D. Mehta, and A.B. Malik. 2007. Dual regulation of endothelial junctional permeability. *Sci. STKE.* 2007:re8. http://dx.doi.org/10.1126/stke.4122007re8

Korhonen, H., B. Fisslthaler, A. Moers, A. Wirth, D. Habermehl, T. Wieland, G. Schütz, N. Wettschureck, I. Fleming, and S. Offermanns. 2009. Anaphylactic shock depends on endothelial Gq/G11. *J. Exp. Med.* 206:411–420. http://dx.doi.org/10.1084/jem.20082150

Kozasa, T., X. Jiang, M.J. Hart, P.M. Sternweis, W.D. Singer, A.G. Gilman, G. Bollag, and P.C. Sternweis. 1998. p115 RhoGEF, a GTPase activating protein for Galpha12 and Galpha13. *Science.* 280:2109–2111. http://dx.doi.org/10.1126/science.280.5372.2109

Kress, M., B. Riedl, and P.W. Reeh. 1995. Effects of oxygen radicals on nociceptive afferents in the rat skin in vitro. *Pain.* 62:87–94. http://dx.doi.org/10.1016/0304-3959(94)00254-C

Li, Q., N.Y. Spencer, F.D. Oakley, G.R. Buettner, and J.F. Engelhardt. 2009. Endosomal Nox2 facilitates redox-dependent induction of NF-kappaB by TNF-alpha. *Antioxid. Redox Signal.* 11:1249–1263. http://dx.doi.org/10.1089/ars.2008.2407

Meigs, T.E., M. Fedor-Chaiken, D.D. Kaplan, R. Brackenbury, and P.J. Casey. 2002. Galpha12 and Galpha13 negatively regulate the adhesive functions of cadherin. *J. Biol. Chem.* 277:24594–24600. http://dx.doi.org/10.1074/jbc.M201984200

Meigs, T.E., J. Juneja, C.T. DeMarco, L.N. Stemmle, D.D. Kaplan, and P.J. Casey. 2005. Selective uncoupling of G alpha 12 from Rho-mediated signaling. *J. Biol. Chem.* 280:18049–18055. http://dx.doi.org/10.1074/jbc.M500445200

Mirza, M.K., Y. Sun, Y.D. Zhao, H.H. Potula, R.S. Frey, S.M. Vogel, A.B. Malik, and Y.Y. Zhao. 2010. FoxM1 regulates re-annealing of endothelial adherens junctions through transcriptional control of beta-catenin expression. *J. Exp. Med.* 207:1675–1685. http://dx.doi.org/10.1084/jem.20091857

Nishida, M., Y. Maruyama, R. Tanaka, K. Kontani, T. Nagao, and H. Kurose. 2000. G alpha(i) and G alpha(o) are target proteins of reactive oxygen species. *Nature.* 408:492–495. http://dx.doi.org/10.1038/35044120

Offermanns, S., V. Mancino, J.P. Revel, and M.I. Simon. 1997. Vascular system defects and impaired cell chemokinesis as a result of Galpha13 deficiency. *Science.* 275:533–536. http://dx.doi.org/10.1126/science.275.5299.533

Okada, M., S. Nada, Y. Yamanashi, T. Yamamoto, and H. Nakagawa. 1991. CSK: a protein-tyrosine kinase involved in regulation of src family kinases. *J. Biol. Chem.* 266:24249–24252.

Orsenigo, F., C. Giampietro, A. Ferrari, M. Corada, A. Galaup, S. Sigismund, G. Ristagno, L. Maddaluno, G.Y. Koh, D. Franco, et al. 2012. Phosphorylation of VE-cadherin is modulated by haemodynamic forces and contributes to the regulation of vascular permeability in vivo. *Nat Commun.* 3:1208. http://dx.doi.org/10.1038/ncomms2199

Potter, M.D., S. Barbero, and D.A. Cheresh. 2005. Tyrosine phosphorylation of VE-cadherin prevents binding of p120- and beta-catenin and maintains the cellular mesenchymal state. *J. Biol. Chem.* 280:31906–31912. http://dx.doi.org/10.1074/jbc.M505568200

Rhee, S.G. 2006. Cell signaling. H2O2, a necessary evil for cell signaling. *Science.* 312:1882–1883. http://dx.doi.org/10.1126/science.1130481

Roskoski, R. Jr. 2005. Src kinase regulation by phosphorylation and dephosphorylation. *Biochem. Biophys. Res. Commun.* 331:1–14. http://dx.doi.org/10.1016/j.bbrc.2005.03.012

Salmeen, A., and D. Barford. 2005. Functions and mechanisms of redox regulation of cysteine-based phosphatases. *Antioxid. Redox Signal.* 7:560–577. http://dx.doi.org/10.1089/ars.2005.7.560

Shan, D., L. Chen, D. Wang, Y.C. Tan, J.L. Gu, and X.Y. Huang. 2006. The G protein G alpha(13) is required for growth factor-induced cell migration. *Dev. Cell.* 10:707–718. http://dx.doi.org/10.1016/j.devcel.2006.03.014

Shi, G.X., K. Harrison, S.B. Han, C. Moratz, and J.H. Kehrl. 2004. Toll-like receptor signaling alters the expression of regulator of G protein signaling proteins in dendritic cells: implications for G protein-coupled receptor signaling. *J. Immunol.* 172:5175–5184.

Shimizu, T., T. Numata, and Y. Okada. 2004. A role of reactive oxygen species in apoptotic activation of volume-sensitive Cl(-) channel. *Proc. Natl. Acad. Sci. USA.* 101:6770–6773. http://dx.doi.org/10.1073/pnas.0401604101

Sivaraj, K.K., M. Takefuji, I. Schmidt, R.H. Adams, S. Offermanns, and N. Wettschureck. 2013. G13 controls angiogenesis through regulation of VEGFR-2 expression. *Dev. Cell.* 25:427–434. http://dx.doi.org/10.1016/j.devcel.2013.04.008

Su, T., X. Li, N. Liu, S. Pan, J. Lu, J. Yang, and Z. Zhang. 2012. Real-time imaging elucidates the role of H2O2 in regulating kinetics of epidermal growth factor-induced and Src-mediated tyrosine phosphorylation signaling. *J. Biomed. Opt.* 17:076015.

Turm, H., M. Maoz, V. Katz, Y.J. Yin, S. Offermanns, and R. Bar-Shavit. 2010. Protease-activated receptor-1 (PAR1) acts via a novel Galpha13-dishevelled axis to stabilize beta-catenin levels. *J. Biol. Chem.* 285:15137–15148. http://dx.doi.org/10.1074/jbc.M109.072843

Vandenbroucke St Amant, E., M. Tauseef, S.M. Vogel, X.P. Gao, D. Mehta, Y.A. Komarova, and A.B. Malik. 2012. PKCα activation of p120-catenin serine 879 phospho-switch disassembles VE-cadherin junctions and disrupts vascular integrity. *Circ. Res.* 111:739–749. http://dx.doi.org/10.1161/CIRCRESAHA.112.269654

Wind, S., K. Beuerlein, T. Eucker, H. Müller, P. Scheurer, M.E. Armitage, H. Ho, H.H. Schmidt, and K. Wingler. 2010. Comparative pharmacology of chemically distinct NADPH oxidase inhibitors. *Br. J. Pharmacol.* 161:885–898. http://dx.doi.org/10.1111/j.1476-5381.2010.00920.x

Wu, X., B. Gan, Y. Yoo, and J.L. Guan. 2005. FAK-mediated src phosphorylation of endophilin A2 inhibits endocytosis of MT1-MMP and promotes ECM degradation. *Dev. Cell.* 9:185–196. http://dx.doi.org/10.1016/j.devcel.2005.06.006

Xiao, K., D.F. Allison, K.M. Buckley, M.D. Kottke, P.A. Vincent, V. Faundez, and A.P. Kowalczyk. 2003. Cellular levels of p120 catenin function as a set point for cadherin expression levels in microvascular endothelial cells. *J. Cell Biol.* 163:535–545. http://dx.doi.org/10.1083/jcb.200306001

Yu, W., S. Beaudry, H. Negoro, I. Boucher, M. Tran, T. Kong, and B.M. Denker. 2012. H2O2 activates G protein, α 12 to disrupt the junctional complex and enhance ischemia reperfusion injury. *Proc. Natl. Acad. Sci. USA.* 109:6680–6685. http://dx.doi.org/10.1073/pnas.1116800109